ERIC R.H. Slag properties and design issues pertinent to matte smelting Electric furnaces. *VII International Conference on Molten Slags Fluxes and Salts,* The South African Institute of Mining and Metallurgy, 2004.

Slag properties and design issues pertinent to matte smelting electric furnaces

R. H. ERIC
School of Process and Materials Engineering, University of the Witwatersrand, Johannesburg

The effect of composition on electrical conductivity (resistivity), viscosity and liquidus temperature of the slags encountered in electric smelting of PGM containing suphide concentrates is reviewed, along with the relationsip between slag composition, slag-matte separation and metal losses to slag. Optimization of slag composition at furnace temperature is attempted on the basis of opposite and parabolic trends of the viscosity-conductivity relationships of the slags. The importance of surface tension of slags is emphasized using available and estimated information which are grouped into a useful correlation. These values are coupled with or incorporated into slag viscosity plots to illustrate the correlation between the two factors, which influence slag-matte separation as well as refractory attack.

The electrode in the slag-resistance furnace is the central factor in the design and operation of the furnace by its role of conveying the smelting power. The obvious parameters are the size and positioning in the slag bath, which are defined by slag resistively, furnace resistance, cell constant and power input. The flow of heat generated by the electrode current determines the energy distribution and furnace dimensions creating viscosity profiles, which in turn affect flow conditions. Thus the flow of slag and matte are discussed in conjunction with the furnace geometry, stirring action of the electrodes, buoyancy and electromagnetic effects. The action of the electric furnace as a settler is discussed. The rectangular furnace is considered as a channel reactor in this analysis, and the action of the electrodes is described to indicate a balanced settling rate in the area of electrode action.

Discussion of the design and production capacity of the electric furnace, with reference to operating current, power input, furnace dimensions and electrode size, are based on considerations derived mainly from slag properties such as its resistively, viscosity and liquidus temperature.

Introduction

The copper-nickel and PGM (Platinum Group Metals) bearing concentrates produced in South Africa are smelted in electric furnaces. The slags obtained in the smelting of these low grade concentrates have relatively high MgO contents, which as a consequence of their high electrical resistivity renders them suitable for sufficient heat generation needed for the smelting process. The other main slag constituents are SiO_2, FeO, Al_2O_3 and CaO. The two main factors in the adoption of electric smelting of these concentrates are the favourable cost of electrical energy in South Africa and the high MgO content of the concentrates, resulting in relatively high operating temperatures in the electric furnace. Moreover, the concentrates do not exhibit excessive variation in the main slag constituents, which are normally greater than 60% by mass. As a result, the grade of electrical furnace matte will also be low, containing 16–18% Ni, 9–11% Cu, 38–42% Fe and 26–28% S with around 600g/tonne PGMs[1,2].

Thus in Cu-Ni matte smelting, the heat is generated by the electrical resistivity of the slag. Then the resistivity of the slag largely determines the rate of production, efficiency of smelting and also the dimensions of the furnace for a desired rate of production. The other slag properties, viscosity and liqiudus temperature, play a decisive role in the flow characteristics, slag–matte separation and the settling of matte particles through the molten bed of slag.

The knowledge of the flow characteristics of slag and matte in the electric furnace is of great importance because the molten slag bed acts as a (i) heating medium for the matte and (ii) as a carrier, that is the settling medium of the molten matte droplets released from the concentrate both, of which affect the whole economy of the furnace.

Concerning the material itself, consisting of molten slag through which the matte droplets settle, an obvious constraint is the viscosity of the slag, which affects the surface and interfacial tensions. The viscosity of the slag is a function of temperature or heat distribution in the melt along with composition. With respect to the matte droplets, there are three factors that ultimately define the economy of the separation: their rate of liberation from the concentration, their size and rate of settling, this conversely being a function of size, then slag viscosity and specific gravity relationships.

In electric matte smelting furnaces the efficiency of operation also depends on the soundness of the electrical side of the furnace, as well as on the design of the furnace as a reactor to promote the separation and settling of the matte through the slag as mentioned above. Thus the movement of the slag bath as a function of furnace geometry, along with the stirring action of the electrodes in association with buoyancy and electromagnetic effects, is of prime importance. In essence, the electric furnace acts as a separator and settler. The design of the furnace must take this double task, into account. The exact knowledge of the

Table I
Typical composition of concentrates and furnace products at large operating plants in South Africa

Materials	PGM g/tonne	Ni	Cu	Fe	S	Basicity $\frac{CaO+MgO}{SiO_2}$	FeO	CaO	MgO	Al_2O_3	SiO_2
		% (Mass)					(Average mass percentage)				
Concentrate	110–150	3.5–4.0	2-2.3	15.0	8.5–10			3	11	6	3.9
Furnace matte	500–600	16–18	9–11	38–42	26–28						
Converter matte	1800–2000	47–48	27–28	1–2	20–21						
Furnace slag Plant I	5.54	0.10	0.06–0.08		0.27	0.74	20	15	15	6	41
Furnace slag Plant II		0.10	0.10			0.55	23	8	18	3	4

behaviour and interaction of the slag and the descending matte droplets must be known.

It is quite clear that, based on the above mentioned discussion, the prime factor in electric matte smelting is the characteristics of the slag, which is derived from the feed materials. The aim of this paper is to provide an overview of these issues based on laboratory scale experimental research, actual plant data, plant measurements and observations, both fundamental and empirical calculations and own experience. Some details of these investigations were individually presented and published as technical/scientific papers[3-9] over a period of six years from 1994 to 2000. Therefore such details will not be presented here in this limited paper. Table 1 is included here to give an idea of the typical composition of concentrates, matte and slags encountered in electric smelting of PGM concentrates in South Africa.

Viscosity, resistivity, liquidus temperature and slag optimization

The slag contents varied in the following ranges: CaO 13–19%, MgO 13–19%, FeO 14–26%, SiO_2 38–46%, Al_2O_3 5%. The basicity ratios, expressed as B = (CaO% + MgO%) / (SiO_2%) were in the range 0.6 to 1.0 and CaO/MgO ratio in the range 0.8 to 1.2. The resistivities were measured at 50º and 100ºC above liquidus temperature, the viscosity at 1400ºC and 1450ºC. Figure 1 is a typical case illustrating the effect of basicity ratio, CaO to MgO ratio, and MgO content on the resistivity, viscosity and liquidus temperature of slag group II (FeO 20%, CaO 16%, Al_2O_3 5%). Increasing MgO content while decreasing resistivity and viscosity significantly will increase the liquidus temperature.

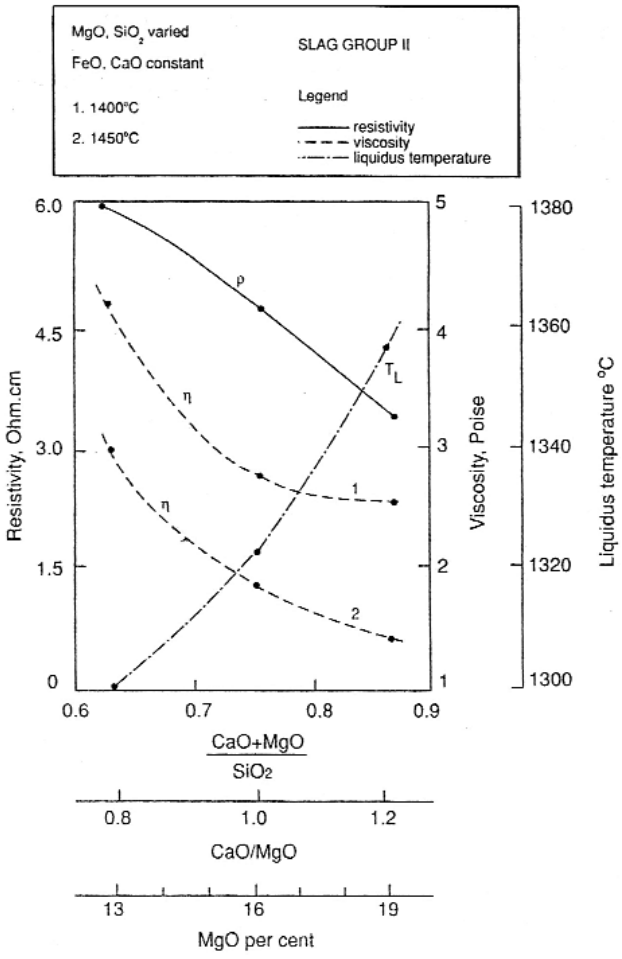

Figure 1. Effect of basicity, CaO/MgO ratio and % MgO on resistivity, viscosity and liquidus temperature of slags

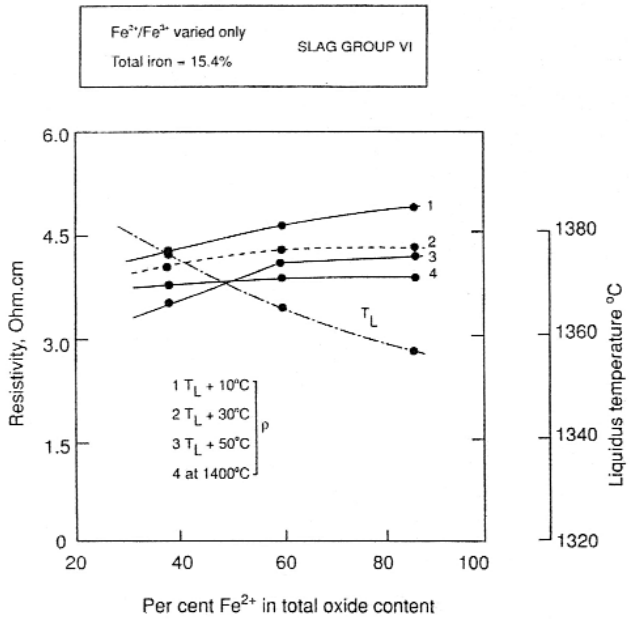

Figure 2. Effect of Fe^{2+}/Fe^{3+} ratio on the resistivity and liquidus temperature of slags

Table II
Comparison of viscosity and electrical conductivity of synthetic and plant slags at 1400°c

Plant Slags				Synthesis Slags					
Variation in plant slag composition (mass %)				Conduct-range (ohm^{-1} cm^{-1})	Viscos. range (poise)	Equiv. synth-etic slag group	Slag constitu. upon which comparis. is based	Conductiv. range (ohm^{-1} cm^{-1})	Viscosity range (poise)
CaO	MgO	SiO_2	Fe_{total}						
16.0	12.8 – 14.8	40.1 – 41.9	15.3	0.217–0.238	3.10–3.40	II	MgO SiO_2	0.195–0.218 0.255–0.271	3.10–4.10 2.55–2.52
16.1 - 18.1	16	40.1 – 41.9	12.2–16.5	0.217–0.238	3.10–3.40	IV	Fe_{total} CaO SiO_2	0.200–0.255 0.226–0.295 0.272–0.300	2.65–3.66 2.35–2.75 2.30–2.55
16	12.8 – 14.8	40.1 – 41.9	12.2–16.5	0.217–0.238	3.10–3.40	V	Fe_{total} SiO_2	0.219–0.237 0.217–0.295	2.48–3.45 1.94–2.35

The effect of CaO on slag properties, except viscosity, follows the same trend but is much less pronounced, which also applies to the effect of FeO, especially when basicity and MgO content is constant.

Figures 2 and 3 illustrate the effect of Fe^{2+}/Fe^{3+} ratio on all three slag properties. As seen, the increase in Fe^{2+} content has limited effect on the resistivity where as viscosity slightly decreases with decreasing Fe^{2+} down to about 50% Fe^{2+} (in total iron oxide content), but then a further decrease in Fe^{2+} brings in a noticeable increase in viscosity. The liquidus temperature drops steadily as Fe^{2+} increases. Table II compares data on plant and synthetic slags. From the comparison it becomes evident that caution will have to be exercised in projecting the results of laboratory investigations on synthetic slags with regard to their effect of the various slag forming constituents onto their possible effect in actual slags.

The quantitative expression of the slag properties mentioned above was achieved by neural net modelling[9] and activation energies were calculated for conduction and viscosity, which were in the 67 to 159 kJ/mol and 125 to 209 kJ/mol respectively. Since electrical conductivity and viscosity exhibit two opposite trends on the change of composition in a given slag system, their interaction as a function of slag composition might serve as a basis for the type of slag for optimizing electric furnace performance.

One way of approaching this goal is to utilize the graphical representation of the viscosity-conductivity curves whereby the point of intersection of the two, in most cases roughly parabolic curves, projected to the composition axis may be regarded as the desirable slag composition. Figure 4 serves as an illustration of the concept. This procedure was used to compare suggested optimum slag composition with actual plant slags. From the comparison it appeared that the FeO and CaO contents of the plant slags were in the optimum range, while MgO was lower by about 2 to 3 percent and SiO_2 by about 1.5–2.0%. The viscosity range of plant slags was higher than that indicated by calculations. On the other hand, the difference between relevant conductivity values was

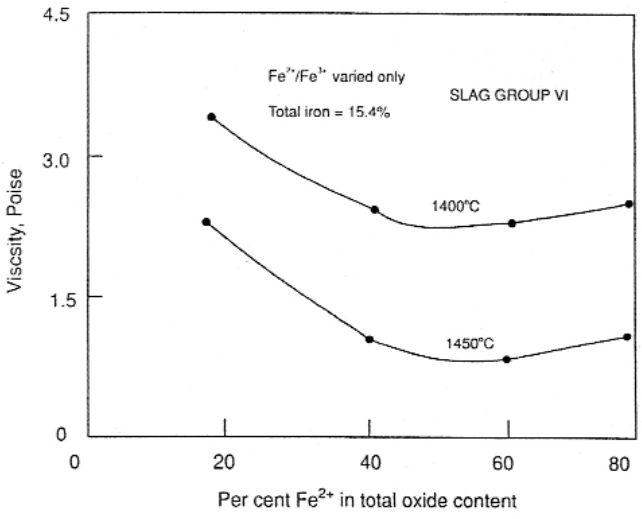

Figure 3. Effect of Fe^{2+}/Fe^{3+} ratio on the viscosity of slags.

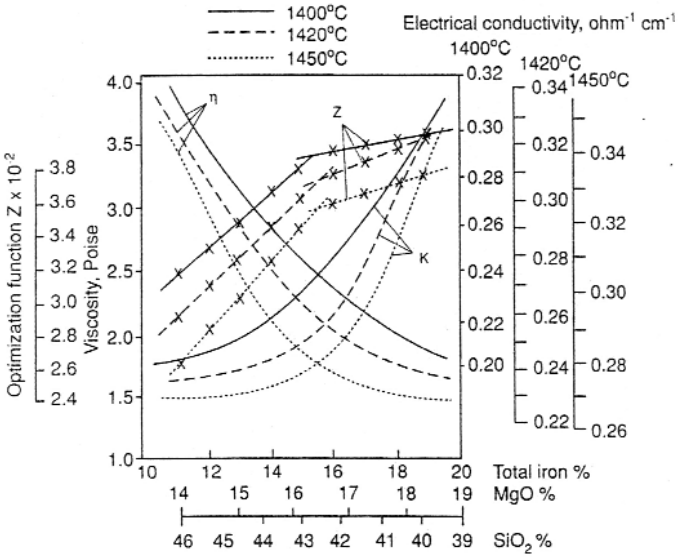

Figure 4. Viscosity-conductivity relationship of Group V slags together with optimization function as a function of total iron, %MgO and %SiO_2

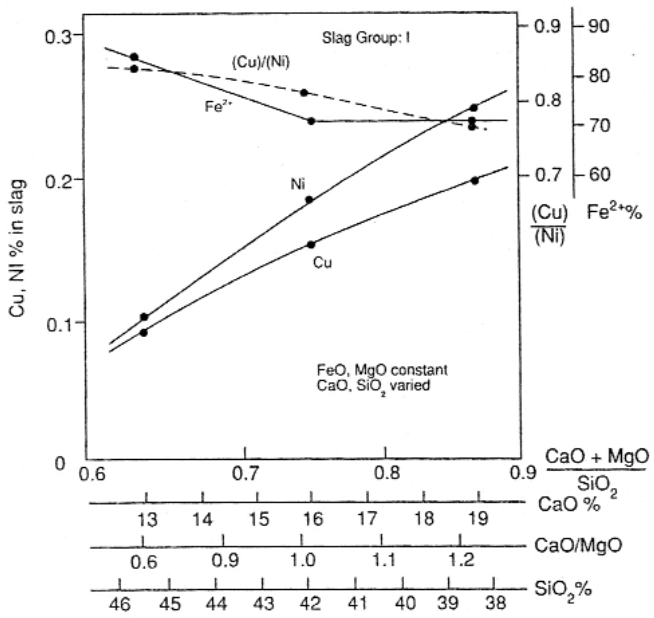

Figure 5. Effect of basicity, %CaO, CaO/MgO ratio and %SiO_2 on Cu and Ni losses to slag

insignificant, indicating the bias towards electrical side of the operation in working plants. It was found that the following equation could be used to express analytically the relationship among viscosity, conductivity and slag composition[3].

$$Z = erf\left(\frac{C_A}{2\sqrt{k}}\right)of\left(\frac{C_B}{2\sqrt{k}}\right) + erf\left(\frac{C'_A}{2\sqrt{\eta}}\right)erf\left(\frac{C'_B}{2\sqrt{\eta}}\right) \qquad [1]$$

In Equation [1] Z is the optimization function (or number), k is conductivity, η is viscosity, C_A and C_B are concentrations of slag constituents that affect the conductivity most, and C'_A and C'_B are the concentrations of the slag components that affect the viscosity. Figure 4 includes plots of Z function, which show a definite infliction point at the optimum slag composition as defined by the intersection of the viscosity-conductivity curves. Here the C_A and C_B referred to concentrations of MgO and FeO for both conductivity and viscosity.

Metal losses to slag, matte-slag separation and settling

Metal losses in furnace slag can be attributed to two main reasons: physical entrapment of matte prills in the course of their settling through the slag and chemical/electrochemical dissolution. The mode of studying the nature of the true extent of the losses has an important bearing on how the experimental data can be related to, or would be representative of the losses occurring in practical furnace operation.

Extensive test work was conducted in our laboratories for electric smelting of PGM containing copper-nickel concentrates of South Africa using the slag composition ranges mentioned earlier[3]. The viscosity of the slags investigated varied from 1.5 to 4.0 poise at 1400ºC which, on the basis of Stoke's law, would limit the matte particle/prill size to 15μm for the estimated terminal velocity of 2.8 X 0^{-4} cm/s to reach the bottom of the melt under our experimental conditions. Tests were also conducted using various slag compositions to study the

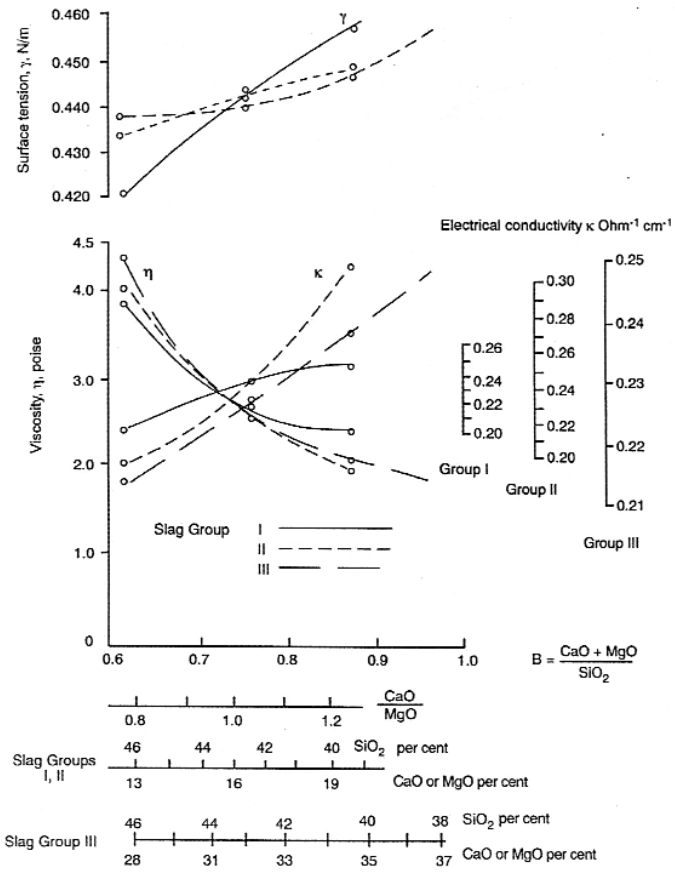

Figure 6. Viscosity, electrical conductivity, surface tension and slag composition relationship at 1400ºC for slag groups I,II,III

effect of FeO and the basicity ratio on matte-slag separation.

The brief summary of results include the following: (i) the copper and nickel solubility increases with the increase of the basicity ratio, CaO and MgO contents of the slag, (ii) at constant CaO/MgO ratios in the slag, even with increasing basicity, the metal losses are reduced, (iii) keeping the FeO and SiO_2 contents constant in the slag, the substitution of MgO with CaO reduces metal losses, and (iv) the relationship between slag composition and slag-matte separation and settling depends primarily on the basicity ratio and the FeO content of the slag.

High basicity ratios coupled to low FeO contents are detrimental to separation of the two phases. It appeared that a minimum of around 12% FeO is required for reasonable separation of matte and slag. Even when iron oxide content of the slag is adequate, high basicity ratios could lead to unsatisfactory separation and settling of matte prills, mainly due to a rise in liquidus temperature and hence viscosity of the slag brought about by the enhanced CaO and MgO and reduced SiO_2 contents of the slag[3,4]. Figure 5 is a typical plot for some of the results obtained on metal losses to slag.

Obviously the main controlling factor in the settling rate of matte prills is the viscosity of the slag, which also affects to a large extent the coalescence of the prills. An increase in the prill size leads to increased settling viscosity by considering their terminal velocity in the Stoke's law. In view of the Reynolds numbers, charactertic to the movement of the liquid phases in electric furnaces, as calculations indicated, the Stoke's law could safely be used.

Apart from viscosity, the rate of settling could be

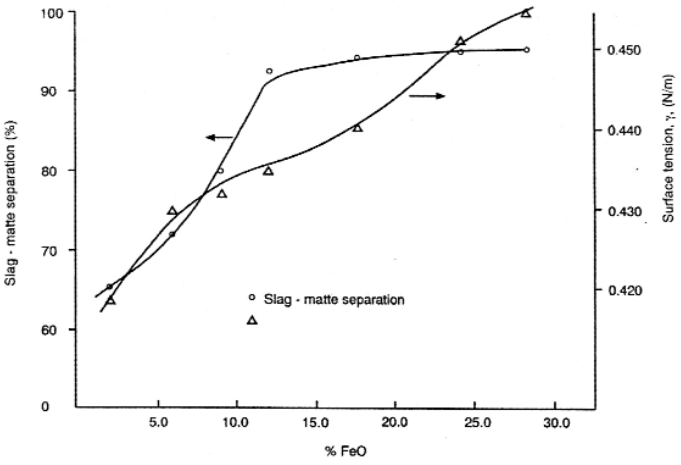

Figure 7. Slag-matte separation and surface tension of slag in smelting
(CaO+MgO)/SiO_2=0.74–0.80
%Al_2O_3=5%

markedly affected by the interfered tension between the matte and slag. When the interfacial tension between matte and slag is low, the matte is wetted by the slag and the settling velocity of matte prills is reduced. The tendency for coalescence should increase with increasing interfacial tension, but the ability of the prills to coalesce when in contact will also depend on viscosity. The lower the viscosity, the better the tendency to coalesce. Due to severe lack of data on interfacial tensions pertinent to the slag-matte systems encountered in electric furnace a rather indirect approach was adopted by using surface tensions available. The details of this approach were outlined in an earlier publication[8] and thus will not be repeated here. At 1400ºC, the expression used in the calculation of the surface tension of slag in dynes/cm is:

$$\gamma = 570X_{Feo} + 285X_{SiO_2} + 640X_{Al_2O_3} + 614X_{CaO} + 512X_{MgO} \quad [2]$$

Figure 6 illustrates the results of such calculations for some of the slags studied. The magnitude of surface tension in the slags under operating conditions is between 420 and

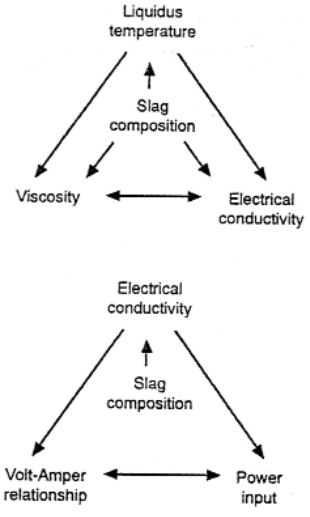

Figure 8. Correlation of various parameters in the operation of the electrical smelting furnace

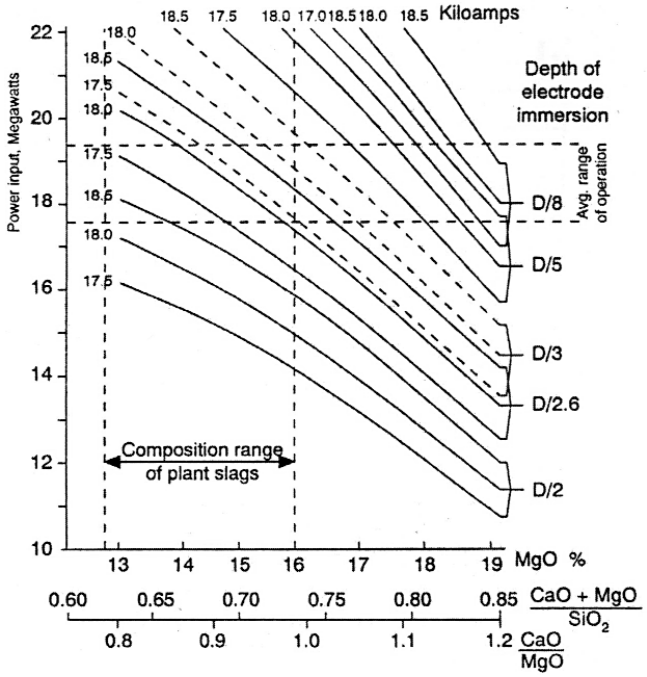

Figure 9. Effect of slag composition upon various characteristics of furnace operation. Slag Group II, temperature 1400ºC

460 dynes/cm (0.42–0.46 N/m) and tend to increase with total iron, CaO, MgO and basicity ratio. Increasing SiO_2 content, in agreement with literature, decreases the surface tension. The figure also contains electrical conductivity and viscosity values of the same slags to show the general trends.

Figure 7 summarizes the relationship between surface tension of the slags and slag-matte separation. The increase in the FeO content in the slag of constant basicity ratio and Al_2O_3 content brings about a very substantial slag-matte separation up to about 12% FeO level. There is a less spectacular change in surface tension apart from the starting section of the plot in which the FeO content changes from 2 to 6%. Nevertheless, there appears to be a direct relationship between matte-slag separation efficiency and surface tension of the slag.

Current area heat flow in the slag

The heat in the electric furnace is generated by the current passing through the slag according to the $Q = I^2R$ formula, thus the slag resistivity is of prime importance in the overall efficiency of the operation.

As a control parameter it stipulates the distance between the electrode and matte surface in the molten slag and, consequently, serves also as a design parameter for the electrode geometry, i.e. diameter, spacing of electrodes and depth of electrode immersion. Thus the position of the electrode in the melt determines the mode of heat dissipation, which gives the smelting area.

Since the depth of the molten slag layer is decisive in the settling of matte prills, the electrode position of the slag has important bearing upon the whole economy of the furnace operation. Viscosity affects the flow quality of the slag and the settling of matte prills. Unfortunately, the conductivity and viscosity properties of the slag are opposite to each other.

Thus while the decrease in conductivity would be beneficial from a smelting point of view, the simultaneous increase in viscosity tends to diminish the gains that would

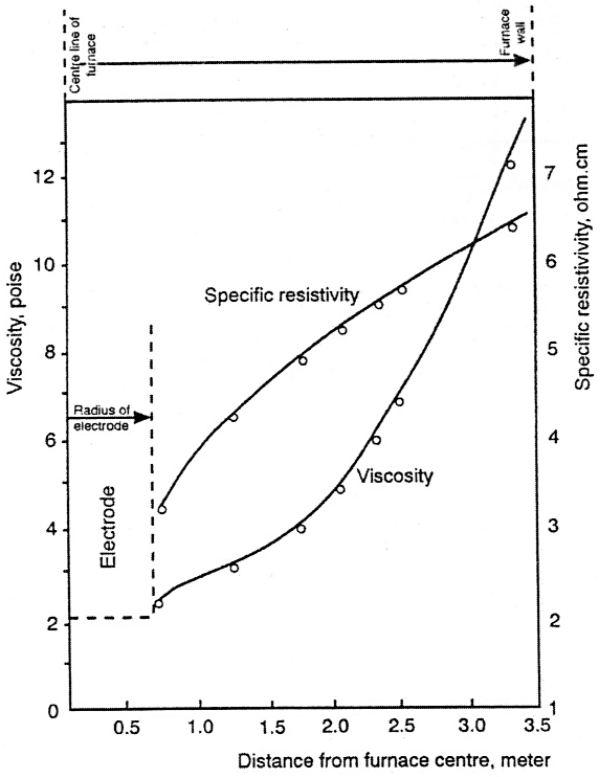

Figure 10. Horizontal gradient of viscosity and specific resistivity in the slag bed between the electrode surface and the furnace wall

ensue from the increase in the resistivity. The liquidus temperature of the slag should be as low as possible to diminish radiation heat losses but must also result in acceptable viscosities. Furthermore, low liqiudus temperatures will cause less refractory lining wear. The relationship among the various slag parameters is depicted in Figure 8.

From a furnace design point of view it is important to determine the voltage-current relations that influence electrode size and spacing, then furnace dimensions. In this context, the resistance (leading to furnace resistance) has to be evaluated:

$$R_s = \rho_s k \qquad [3]$$

Here R_s is slag resistance (assumed primarily ohmic), ρ_s is slag resistivity (ohm-cm) and k is the cell constant for a given electrode geometry (cm^{-1}). Several significant attempts have been made in the past to correlate resistivity with various parameters, the most often used one being the electrode diameter D_e. It is not the intention of this paper to review these since they will take significant mathematical manipulations and space. These have been briefly reviewed in an earlier publication[5] along with the method adopted by the current author.

Then, in general, to estimate the effect of slag composition on furnace load, the furnace resistance was calculated using equation [3] and using the specific slag resistivity data obtained in laboratory measurements. Finally, the current and power were evaluated by standard relationships[5].

An illustrative example is shown in Figure 9 where electrode diameter D_e = 1.25 m, electrode spacing S = 2.7 De = 3.375m, slag depth H = 1.40m and depth of electrode immersion p = 0.5 m based on slag resistivity data. Figure 9

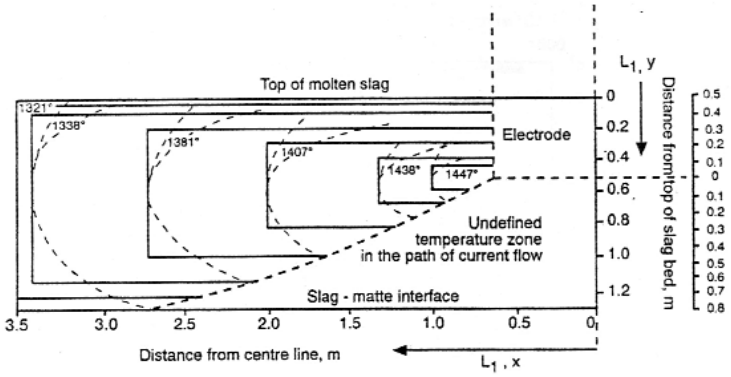

Figure 11. First order Ritz profile of two-dimensional heat distribution in the molten bed of slag

shows the effect of slag composition upon the power input at various depths of electrode immersion with furnace currents 17.5, 18.0 and 18.5 kA as parameter. Slag temperature was taken as 1400ºC.

The change of slag temperature has a marked effect on both operating current and power input rates due to change in the resistivity of the slag upon temperature variation. Naturally, the position of the electrode in the molten slag also changes. Then it is absolutely necessary to have temperature-resistivity relationships, preferably in a sound analytical format, i.e. the neural-network modelling mentioned earlier. Quite obviously, a change in slag composition will also change the position of the electrode as can be seen from Figure 9.

Thermal conditions in an electric furnace are extremely complex, so that a quantitative and practical treatment of the system requires a number of simplifying assumptions, such as steady states conditions and heat transfer occurring equally in all directions. The radial (horizontal) heat distribution around an electrode is important in that it determines the spacing of the electrodes and thereby the general furnace geometry. In the present analysis, as a conservative estimate based on actual plant measurements carried out close to the periphery of the electrode tip, a temperature of 1500ºC is assigned to the slag layer regarded as a disc in continuation or extension of the electrode.

Practical temperature measurements on operating furnaces indicated a region extending upwards from the level of the electrode tip, in which the temperature gradient is relatively small (25º to 40ºC). Based on this finding, the system can be visualized as the heat being distributed in a thick plate from a cylindrical heat source embedded into this plate. Since the interest is the radial flow of heat, the temperature drop along the lower surface of the plate is investigated.

The temperature distribution estimated around the electrode, the details of which can be found elsewhere[5] enables the determination of the resistivity and viscosity profiles (using the data on resistivity and viscosity of the slag as a function of temperature) in the electrode area. A typical plot is shown in Figure 10. The tendency is that with the increase of temperature, the gradients of both viscosity and resistivity become steeper, which will give rise to buoyancy effects. These forces will tend to disperse the settling matte prills into further regions of the slag bath and away from the electrodes, rendering the pattern of their settling much less, if at all, predictable.

The possibility of extending the simple one-directional heat flow concept into a two dimensional one can be attempted. Here again the details are omitted but can be found elsewhere[5]. Again a typical result is illustrated in Figure 11 in the form of a Ritz profile of two-dimensional heat distribution. The dotted lines in the figure extending beyond the boundaries of the rectangular profiles represent approximate temperature boundaries when the true parabolic profiles become distorted by the movement of the slag as a result of buoyancy forces and electromagnetic effects. These dotted profiles are based on actual plant measurement. The temperature profile between (i) the top of the slag bed and the level of the electrode tip and (ii) the level of electrodes tip on slag/matte interface was obtained by applying the thermal conductivity of two-phase mixtures.

Actual temperature measurements carried out in the slag bath of a working unit indicated the existence of an extensive slag layer (35–40cm) in a vertical direction in which the temperature variations were limited. Selecting the proper boundary conditions (T = 1300°C at the slag/burden interface, T = 1280°C at the slag/matte interface, and T_{max} = 1460°C), the vertical temperatures profiles can be estimated[5] as illustrated in Figure 12. The circles and the triangles in the figure represent calculated values, while the measured results are denoted by crosses. These were obtained at a rather high electrode position (0.2-0.3 m), while the calculations relate to an optimum electrode level, about 0.5 m (De/2.5) with De = 1.25 m. The broken curves represent suggested conditions for high and low electrode positions. It is clear how in high electrode position the hot zone is shifted upwards to the slag top, cooling down the bottom, and in low electrode position the hot zone is shifted downward to overheat the matte surface, cooling down the top of the slag as the electrode moves.

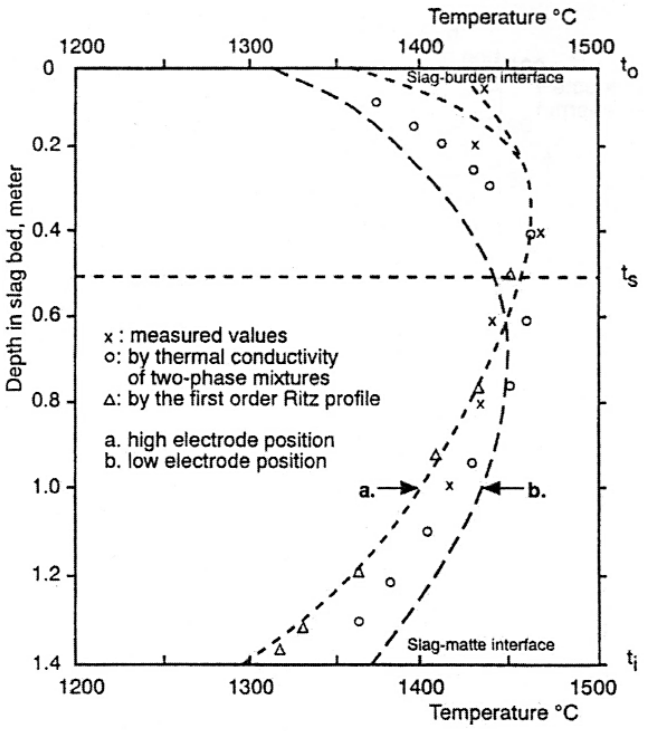

Figure 12. Comparison of measured and predicted vertical temperature gradients

Flow and settling phenomena

In a rectangular furnace (six electrodes in line) with length (L) to width (W) ratio of around 4, the slag flow can be regarded as channel flow[7]. The velocity is mainly in the laminar flow range due to the large volume of melt involved and the evenly distributed feed along the entire length of the furnace. The laminar nature is modified to various extents by the action of the series of electrodes positioned in the centre line of the melt and by periodic addition of converter return slag.

However, as calculations indicated[7], the action of these factors does not alter substantially the laminar flow pattern at the power densities used. The calculations are rather involved and beyond the slope of this presentation but can be found elsewhere[6, 7]. The important results are outlined in the following for a typical furnace of length: 26 m, width: 7 m, with average slag depth: 1.5 m, slag tapped per hour: 21 tonnes and average slag density: 2.8t/m^3 at 1400°C. The average residence time of the slag in the furnace is calculated as 36.5 h. The average velocity of the slag from operating data is then 0.712 m/h (or 0.02 cm/s). The same velocity can be calculated as 0.686 m/h purely from theoretical calculations involving Navier-Stokes equation. The small difference of 3.6% would indicate that the action of electrodes brings about a modest increase in the slag flow velocity.

On the other hand, the velocity of the slag moving radially away from the surface of the electrode on top of the slag melt was calculated as 0.2 cm/s by measurements under operating conditions. This value is an order of magnitude higher in the transverse flow direction than that obtained in the axial bulk flow direction of the bath, yet its disturbing effect upon the general flow pattern appears insignificant in the particular furnace geometry.

Based on experimental data (both from the laboratory and plant measurements), statistical assessment of size distribution of matte prills entrapped in the slag was carried out. The obtained values were converted into actual weights as represented by the various size fractions[4, 7]. The weight distribution is inversely proportional to the number of particles (prills) and increases with increasing size range. Prills up to 200μm size represent only about 10% of the total matte prill weight, while 90% is made up from the weight of larger prills.

The importance of prill coalescence as mentioned earlier is apparent from the investigations. In the rather limited temperature range of investigation of the coalescence properties (1350°–1450°C), it can safely be concluded that the temperature gradient of the viscosity of the slag will play a major role in prill coalescence. Nevertheless, this fact further complicates the exact determination of matte settling and adds to the difficulty of adequate dimensioning of settling zones for electric furnaces.

Matte settling and adequate dimensioning is further complicated by the movement of the slag due to (i) buoyancy and electromagnetic effects, and (ii) the stirring action of the electrodes. As mentioned earlier, the difference in temperature between the top (also the bottom) and the highest temperature layer surrounding the lower half of the submerged electrodes, together with the horizontal and vertical temperature gradients create buoyancy effects leading to convection currents in the slag bath.

Using dimensionless Grashoff number (Gr), which takes into account the variations in density and viscosity as well as temperature differences, together with the Prandtl

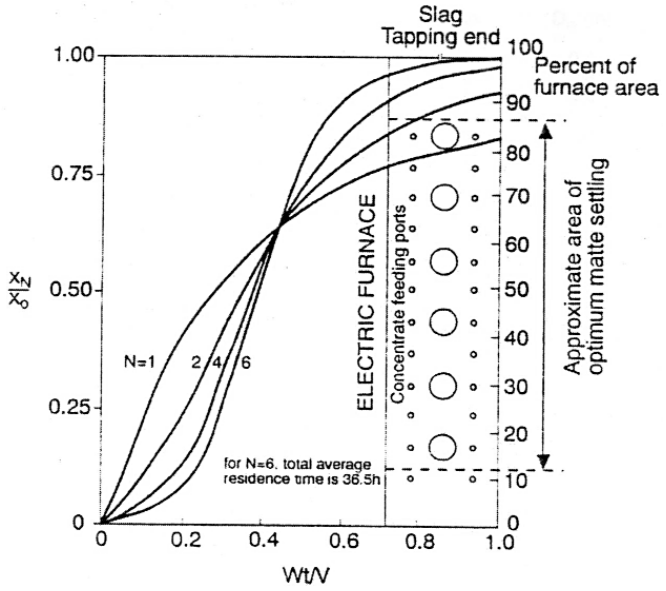

Figure 13. Matte settling in the total length of the electric furnace by the analogy of output from an N tank system of total volume

number (Pr), which correlates viscosity, specific heat and thermal conductivity, the criteria for transition from laminar to turbulent flow in a free convection boundary layer can be determined as their product, known as Rayleigh number R_A (R_A=GrPr).

The laminar flow region corresponds to $10^4<R_A<10^9$ for a wide range of Prandtl numbers (0.00835<Pr<1000). For the specific slags used in electric furnaces, the calculations resulted in Gr = $1.2x10^7$ and Pr = 0.22 to 0.6. Thus R_A was found to lie in the range of 2.64×10^6 to 7.2×10^6 for the present slag system, clearly indicating that the slag will flow under laminar conditions by natural convection.

Based on the above and measured physicochemical properties of the slag, it can be concluded that a considerable degree of slag motion would be by buoyancy force brought about by gradients in slag properties. An analysis of the effect of electromagnetic forces on bath mixing was conducted[7] by using the Reynolds number (Re) and calculating mixing power (due to electromagnetic forces) for the given slag system and furnace dimensions under laminar flow conditions. The mixing power per electrode was calculated as $1.11x10^{-2}$ kW (in unit time).

Even at the highest Re numbers and the smallest friction factors possible, the mixing power was very small. These calculations also showed that the maximum average slag velocity due to electromagnetic effects would be 0.09 m/s compared to 0.712 m/s from the operating data. It can safely be concluded that in six-in-line electrodes furnaces the stirring action comes about mostly by buoyancy, rather than by electromagnetic effects. This point is of considerable practical importance for settling of matte prills. Since fluid flow is largely independent of the effect of the magnetic force field, only the power variations would primarily influence the settling / smelting rate.

However, in three electrode circular furnaces operating at substantially higher power densities, the current density at the interface will be higher and, consequently, the effect of the electromagnetic field far more pronounced. Naturally with a strong increase in resistivity of the slag, at higher temperatures of operation, the electromagnetic force action may increase to a large extent and with this also its stirring effect upon the melt.

The six-in-line electrode furnace can be considered as made of six separate reactors. When these are fed at the same rate with concentrate, provided the stirring effect of the electrodes and the buoyancy forces acting are the same, it is easy to show that the settling and carry-over of the matte prills in their size ranges will also be the same in each unit.

In this rather idealized case of balanced operation, the smelting rate at each electrode is equal with equal quantities of matte and slag produced per unit time in all the units. Naturally, for an equal smelting rate in each reactor, the weight of matte overflowing from one compartment into the other (W_o) end, the rate of recycle is the same. Then from a matte loss point of view, it is only the material balance in the last settling zone that really matters. Then with W_o into the last unit the relationship between the weight of matte tapped (W_t) and that last in the slag (W_s) is given as:

$$W_o = W_t + W_s \qquad [4]$$

The efficiency of smelting, η is:

$$\eta = \left[1 - \left(W_s / W_t\right)\right] x100 \qquad [5]$$

In a somewhat more involved treatment when the unit is regarded as a series of stirred tank reactors, the concentration of matte prills, i.e. the increase (or decrease) in the weight of the settled matte particles can be analysed by the analogy of the change of isotope tracer concentration in the same reactor system. In this instance only the prills released in the first reactor are considered, which follow their way through the entire length of the furnace irrespective of the additional quantities of prills joining the batch obtained in the first reactor. The method adopted is based on the application of differential difference equations, taking into account that the equipment is subjected to step changes in operating conditions. That is, when the composition of the stream changes as it passes through the various process stages, differential terms are added to the finite difference terms[7].

If the number of stirred tanks is N, each with volume v and matte prills of a given size fraction of concentration X_O (kg/m^3) are introduced in the first tank at a rate of Q, then the concentration or the amount of settled matte prills in the Nth reactor X_N will be (total volume of the system = Nv = V = constant, and W is weight):

$$X_N = X_O - X_O e^{-N(Wt/v)} \left[1 + \frac{wt}{v} + \frac{(Nwt/v)^2}{2!} + ... + \frac{(Nwt/v)^{N-1}}{(N-1)!}\right] \qquad [6]$$

The weight increase of settled matte prills on the basis of equation [6] for N = 6 is show in Figure 13. The graph illustrates how the system responds to different values of N. The abscissa represents the ratio: settled volume/total volume of matte prills of given size fraction in time dependent relationship for the total average residence time of 36.5 hours, while the ordinate gives the ratio of settled matte/total introduced matte.

From the plots one may conclude that the most significant increase in the weight of the settled matte takes place between about 2/5th and 4/5th of the time available for settling of a given size range of prills when the total time availability is set by the dimensions of the settler (length, bath levels, taphole position). Further, this would lead to the conclusion that under the conditions of the

electric furnace, the most effective length of the settler would be between about 13 and 86% of its total length. If, for example, prills of a given size range settled so that they would travel from the first compartment to the sixth, the bulk of their settling would come about in reactors 2 to 5. The first increasing then followed by the decreasing trend of removal of matte particles from the slag follows a probability distribution around a maximum as indicated on the graph.

Thus, the importance of the material balance in the last reactor (final settling zone) as an indicator of the total matte loss in the process of settling becomes evident. Figure 13 also includes the appropriate furnace dimensions with the corresponding electrode positions to facilitate the projection of plot N = 6 for settling conditions in a reactor consisting of six stirred compartments, onto an equivalent 6 electrode-in-line furnace. It is believed that this representation is generally valid for these types of furnaces treating similar materials, irrespective of their size. From Figure 13 it will be apparent that in about 75% of the area of the reactor, the release of matte from the concentrate at constant temperature and stirring is, by and large, the same. This of course assumes idealized conditions with equal energy release from the electrodes at their depth of immersion into the slag bath.

Flow conditions in a slag melt stirred by multiple reactors in circular three-triangular electrode furnaces are considerably more complex and quantitative description of matte settling far more difficult than in a channel flow system. This is primarily so because of (i) the greatly reduced space and time availability in the reactor, and (ii) the more concentrated power distribution. No experimental work has been carried out by the present author on these types of units.

Nevertheless, visual observations have been conducted on such furnaces operating in South Africa treating Cu-Ni concentrates containing platinum group metals. The observations on a 5 MVA circular three electrode (0.5 m in diameter, triangular) furnace showed a rather strong boiling-like action around its electrodes when operated at close to full power, which can hardly be conducive to downward flow directions as mentioned in some studies[10]. The effect of the electrode action upon the settling conditions of matte prills is such that, on account of the turbulence the three electrode configuration imparts on slag flow, the prill trajectories will be substantially altered. In actual furnace operation the greatly reduced distance in a 3-electrode circular unit between the electrode and the furnace wall alters also the characteristic settling mode and brings about a high degree of intermixing among the matte prills of different sizes, which causes increases in matte losses to the slag tapped from the furnace.

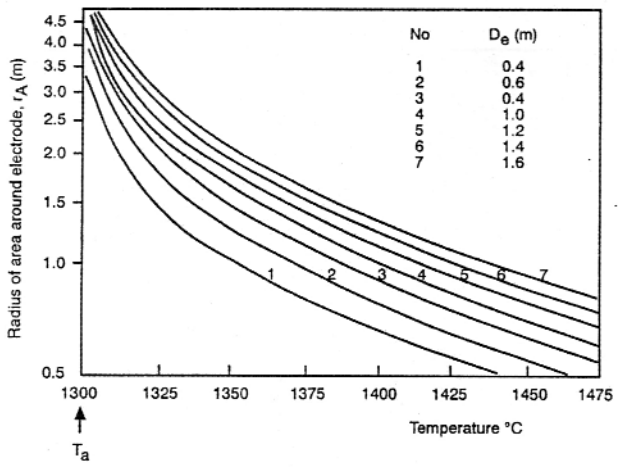

Figure 14. Estimated temperature distribution around electrodes

Dimensioning, design and scale-up considerations

Active area of the electrode refers to the active smelting area, which is by no means equivalent to the melting area, this latter being defined by the liquidus temperature of the slag, which can be considered to vary between 1325° to 1340°C in working furnace slags. However, due to increased slag viscosities near liquidus temperatures, the lower limit of actual slag temperatures would be around 1375°–1380°C. The radial heat flow concept explained earlier can be used, considering that the active zone around the electrodes is also circular, having an area proportional to the diameter of the electrode, to reveal a relationship between electrode diameter and temperature (liquidus temperature). This relationship is shown in Figure 14. According to Figure 14, the radius of the active area around the electrode would be confined to 1.2 to 2.7 m for electrode diameters from 0.4 to 1.6 m.

The furnace width will depend on the electrode diameter and hence the liquidus temperature of the slag. The following simple empirical relationship[6] can be used to determine the furnace width W_f through electrode diameter; D_e:

$$W_f = 6D_e^{0.7} \quad [7]$$

For the relationships between current and electrode diameter, and power and electrode diameter, the following empirical equations can be used:

$$I_{\max} = 20.0D_e^{1.7} \quad [8]$$

$$P = kD_e^{m} \quad [9]$$

In Equation [8] D_e is in cm and I in amps. In equation [9], exponent *m* varies between 1.75 and 2.05 and *k* from 12 to 22 with a change of the depth of electrode immersion between $D_e/2$ to $D_e/5$. For a immersion depth of $D_e/2$ the equation becomes:

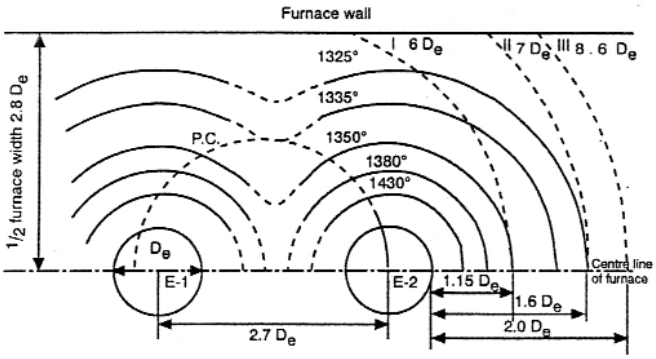

Figure 15. Comparison between radial distribution of heat in furnaces of rectangular (6 electrode in line) and circular (3 electrodes in equilateral triangle) symmetries

$$P = 12.2 D_e^{\,2} \qquad [10]$$

The current density-electrode size relationship can be represented by:

$$_i = 2.95 D_e^{-0.53} \qquad [11]$$

Where Δi is the current density in amp/cm^2. For more specific formulation of the relationship between operating current, current density and electrode size, the following equation can be used:

$$D_e = 2.65x10^{-2}\left(I/\pi D_i\right)^{½} \qquad [12]$$

The empirical relationship between furnace width and area (A) (therefore also length) with the inclusion of the number of electrodes (N_e) is:

$$W_f = \left(\frac{2A}{N_e + 1}\right)^{½} \qquad [13]$$

Another useful direct relationship between furnace length and electrode diameter is the following:

$$L_f = 21 D_e \qquad [14]$$

The following considerations may permit a brief comparison between the symmetry requirements of 3-electrodes-in-triangle circular cross section and 6-electordes-in-line rectangular electric furnaces. As a basis for this comparison, the smelting capacity of the units will be regarded as being equal.

Figure 15 drawn to scale shows the estimated radial temperature distribution around electrode E-1 in the reference rectangular furnace at an optimum electrode immersion depth of 0.5 m = D_e2.5. For this outline the lowest possible limit temperature of 1300ºC was used as a very conservative value for the lower boundary, in which case the radial temperature distribution contours estimated by the Bessel function method with T_{max} = 1500ºC at the electrode surface were indicated in Figure 14. Figure 15 depicts also the dimensions of the electrically equivalent 3-electrode circular furnace with E-2 constituting its second electrode with reference to E-1. P.c is the pich circle (diameter = 3D_e), while dotted line I indicates the distance of the wall from the electrode surface at a furnace diameter of 6 D_e. The distance is 1.15 D_e and as will be seen in the graph, with a radial temperature profile equivalent or similar to that of the 6-in-line furnace, the temperature at this point would be 1350ºC, that is rather high. Two further dotted lines denote the diameter of the round furnace if its wall temperature were to be kept the same as in a rectangular furnace. Line II corresponds with the lowest liquidus, 1325ºC, of the plant slag at a distance of about 1.6 D_e from the electrode surface and represents an internal diameter of 7.7 D_e, while line III gives the diameter of a circular furnace in which the temperature of the slag at the wall would be the same as in the rectangular unit. Thus for the diameter of the thermally equivalent circular furnace $D_{f(c)}$ we can write:

$$D_{f(c)} = 8.6 D_e \qquad [15]$$

Taking an electrode spacing of S = 2.7 D_e, then the diameter of the thermally equivalent circular furnace would be:

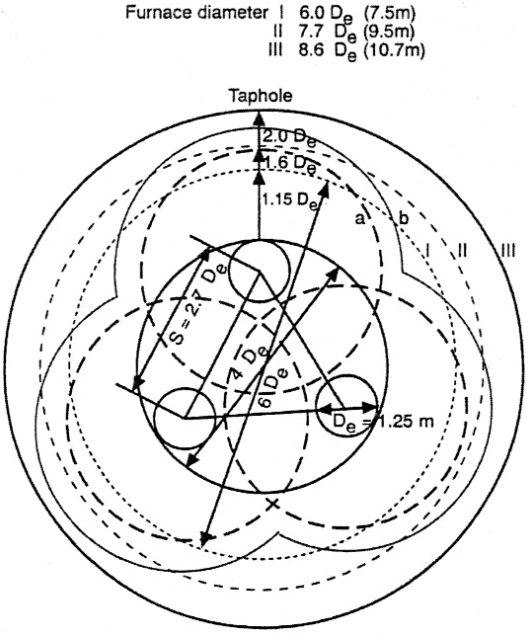

Figure 16. Estimated active areas around the electrodes in equilateral triangular arrangement.

$$D_{f(c)} = 3.2S \qquad [16]$$

The symmetry relations in a rectangular furnace, having electrodes of identical size with regard to width and electrode spacing, are:

$$W_f \;\; 5.6 D_e \;\; 2.1S \qquad [17]$$

These considerations are of prime importance from the point of view of the furnace refractory, which depends to a great extent on the thermal load to which the surface of the wall is exposed. For the three circular furnace diameters discussed above this can be estimated by a method based on the ratio between the pich circle and diameter of the molten slag bath.

Dispensing with any theoretical detail, when r_m is the radius of the melt (molten bath) and r_{pc} that of the pich circle, then the maximum and minimum loads per electrode k_{max}, k_{min} i.e. per phase are given as:

$$k_{\max} = \frac{P_w}{3}\left[\frac{1}{(r_m - r_{pc})^2} + \frac{2}{(r^2{}_m + r_m r_{pc} + r^2{}_{pc})}\right] \times 10^{-2} kVA/m^2 \qquad [18]$$

and

$$k_{\min} = \frac{P_w}{3}\left[\frac{1}{(r_m - r_{pc})^2} + \frac{2}{(r^2{}_m + r_m . r_{pc} + r^2{}_{pc})}\right] \times 10^{-2} kVA/m^2 \qquad [19]$$

For a correct design, by definition k_{min}/k_{max} must be equal or greater than 0.9. Considering the furnace diameters discussed above, the maximum power in each would be 19.3 MW, then with the additional data on D_f we obtain the values for k_{min}/k_{max} as Case I 0.60, Case II 1.03, Case III 0.85. The results clearly indicate that in Case II and III the heating of the wall will be comparatively even and the

design adequate. In Case I, from a heat economy point of view, the design of the furnace would not be satisfactory.

In three-electrode circular furnaces the interaction of the electrode is more intensive and the buoyancy effects, enhanced by electromagnetic forces, exert a further strong hindering effect on matte settling. Figure 16 indicates the relationship for furnaces of different size, I denoting the electrically equivalent 6-in-line furnace of 6 D_e diameter while II and III respectively the minimum (7.7 D_e) and the equivalent 8.6 D_e diameters from a thermal requirement standpoint, as calculated from the relevant working or active area diameters (a) and (b). The latter represents the liquidus temperature as a boundary condition while a) would correspond to about 1385–1390ºC slag temperature.

From a matte settling point of view, the distance available for settling depends to a large extent on the location of the tapholes. They may be situated either opposite to the electrodes or in between two adjacent electrodes when these are in a 3-triangular position. If the matte particles were released in the bulk at the electrode surface, the distance available for settling would be between this point and the furnace wall. By calculation for I this would be 1.44 m, for II 2.0 m and for III 2.5 m, which are rather short distances with very limited settling affordabilities.

Alternatively, the tapholes on the round furnace could be positioned in between the electrodes. In this case, as indicated in Figure 16, the tapholes would be largely beyond the active area of the electrode, assuming quiescent flow conditions. However, as indicated by the graph, it is only about 1 D_e, which is far from being adequate to bring about substantial improvement in matte settling.

In the foregoing assessment, equal slag depth (1.4 m) was assumed for all circular furnaces, which would mean considerably reduced holding capacities as compared to a standard rectangular furnace having 1.25 m electrode diameter. For equal capacities, which are equivalent to equal retention times, the depth of the slag bed for the 7.7 D_e furnace diameter should be 2.5 m and for the 8.6 D_e size about 2 m. This would secure close to equivalent matte settling conditions compared to the rectangular unit.

However, the specific hearth resistance for a three-electrode furnace is given as:

$$\rho_H = R\pi D_e = \frac{U}{I\sqrt{3}}\pi D_e \ \ ohm\ cm \qquad [20]$$

Therefore the current will be $\sqrt{3}$ times that of the 6-in-line units, i.e. in relation to a, say, 18.5 kA in rectangular furnace, 32 kA. Then electrode diameter would be in the 1.5 to 1.6 m range, requiring a safe furnace diameter of minimum 12.5–13.0m.

Conclusions

An overview of slag properties pertinent to electric smelting of Cu-Ni concentrates containing PGMs is provided in relation to slag optimization with respect to resistivity and viscosity, metal losses, matte-slag separation and settling. Current and heat flow in the slag is assessed in conjunction with fluid flow and settling phenomena.

Using all the above, dimensioning, design and scale-up issues were considered for electric smelting furnaces with respect to six-in-line rectangular and triangular circular furnace geometries. It must be emphasized that this overview is mostly based on simplified, somewhat ideal conditions and thus must be treated more as a guideline.

Acknowledgments

The author expresses his sincere gratitude and respect to late Professors D.D. Howart and A.A. Hejja who assisted him to enter into this field and provided some of the data for the complex calculations required by this long-term research.

References

1. MOSTERT, J.C., and ROBERTS, P.N. Electric Smelting at Rustenburg Platinum Mines Ltd of Nickel-Copper Concentrates containing Platinum group metals. *J.S. Afr. Inst. Min. Metall.*, vol. 73, 1973. pp. 290–299.

2. NEWMAN, S.C. Platinum. *Trans. I.M.M*, vol. 82, 1973. pp A52–A68.

3. HEJJA, A.A., ERIC, R.H., and HOWAT, D.D. Electrical Conductivity, Viscosity and Liquidus Temperature of Slags in Electric Smelting of Copper-Nickel Concentrates. *Proceedings of 1994 EPD Congress, San Fransisco*. Warren, G.W. (ed.). Warrandale, Pennsylvania. TSM, 1994, pp. 621–640.

4. ERIC, R.H., HEJJA, A.A., and HOWAT, D.D. Metal losses to the Slag and Matte-Slag separation in electric smelting of Copper-Nickel Concentrates. *Proceedings of 1994 EPD Congress, San Fransisco*. Warren, G.W. (ed.). Warrandale, Pennsylvania, TMS, 1994, pp. 641–656.

5. ERIC, R.H., and HEJJA, A.A. Dimensioning, Scale-up and Operating Considerations for six electrode Electric Furnaces Part I: Current and heat flow in the slag. *Proceedings of 1995 EPD Congress, Las Vegas*, Warren, G.W. (ed.). Warrandale, Pennsylvania. TMS, 1995, pp. 223–238.

6. ERIC, R.H. and HEJJA, A.A. Dimensioning, Scale-up and Operating Considerations for six electrode electric furnaces Part II: Design and Scale-up considerations for furnaces treating PGM-containing copper-nickel concentrates. *Proceedings of 1995 EPD Congress, Las Vegas*. Warren, G.W. (ed.) Warrandale, Pennysilvaia, TMS, 1995, pp. 239–257.

7. HEJJA, A.A., and ERIC, R.H. Flow and Settling phenomena in matte smelting electric furnaces. *Proceedings of 1996 EPD Congress, Anaheim*. Warren, G.W. (ed.) Warrandale, Pennsylvania, TMS, 1996, pp. 27–41.

8. Hejja, A.A,. and Eric, R.H. Aspects of slag optimisation in smelting of Cu-Ni sulphide concentrates. Proceedings of 1997 EPD Congress, Orlando. *Mishra, B. (ed.) Warrandale. Pennsylvania, TMS*, 1997, pp. 179-192.

9. ERIC, R.H., HEJJA A.A., and Reuter, M. Modelling of conductivity and viscosity of copper-nickel smelting slags using neural nets. *Proceedings of 9th International Metallurgical and Materials Congress, Istanbul*. Kayali, E.S. *et.al.* (eds.). Ankara, Turkey. Chamber of Metallurgical Engineers, 1997, pp. 1001-1007.

10. JENSEN, V.G., and JEFFREYS, G.V. *Mathematical Methods in Chemical Engineering*: New York, N.Y. Academic Press, 1963, pp. 338–341.